

MICROMACHINED STIMULATING ELECTRODES

Quarterly Report #3

(Contract NIH-NINDS-N01-NS-2-2379)

April - June 1993

Submitted to the

Neural Prosthesis Program

National Institute of Neurological Disorders and Stroke
National Institutes of Health

by the

Solid-State Electronics Laboratory

Bioelectrical Sciences Laboratory

Department of Electrical Engineering and Computer Science
University of Michigan
Ann Arbor, Michigan
48109-2122

August 1993

MICROMACHINED STIMULATING ELECTRODES

Summary

During the past quarter, research under this program has gone forward in a number of areas. Passive probe fabrication has continued with new mask sets and probes for both external and internal users. Continuing problems with iridium stress and adhesion are being encountered on an intermittent but significant basis and are being investigated with the hope of understanding and eliminating them once and for all. The design of a mask set for probes aimed at optimizing tip shape for ease of insertion and for minimum tissue damage along the tracks has been completed, and the probes are now in fabrication. This set includes 10 different designs featuring a variety of tip angles and processes. Single probes, three-shank probes, and ten-shank probes are included along with strain gauges mounted on some shanks for a direct measurement of entry forces. In parallel with these activities, work has gone forward to improve our external instrumentation for use with the probes. A visualization system has been implemented to enable cortical depression to be recorded, and all of the associated instrumentation for real-time interactive experiments in recording, stimulation, and strain-gauge monitoring has been converted to a LabView-based system. Penetration studies are expected to start in early October.

Using test results from STIM-1 and from STIM-2 circuit chips fabricated at the MOSIS foundry, we have corrected the process/design problems associated with STIM-1 and several minor design problems associated with the STIM-2 circuitry. During the past term, a chip containing the STIM-2 probes was designed, and the masks were fabricated. This chip contains modified layouts of STIM-1a (four-shank, 16-channel bipolar) and STIM-1b (two-shank 16-channel monopolar) as well as three versions of STIM-2: an eight-shank version, an eight-shank folding version, and a 16-shank version. All of the STIM-2 probes use the same circuitry, which implements 8 channels and a 64:8 front-end selector that allows those channels to be coupled to 64 iridium sites. The folding version uses slotted ribbon cables between the probe shanks and the circuitry to maintain a low profile above the cortex for chronic studies. All probes are designed for use with side-mounted ribbon cables. The masks for these devices have been received, and the STIM-2 probe wafers are currently in fabrication. The first prototypes are expected in October. In parallel with these activities, the circuitry for STIM-2 has been successfully operated with our external interface system, confirming the correct implementation of the interface protocols and other logic.

MICROMACHINED STIMULATING ELECTRODES

1. Introduction

The goal of this research is the development of active multichannel arrays of stimulating electrodes suitable for studies of neural information processing at the cellular level and for a variety of closed-loop neural prostheses. The probes should be able to enter neural tissue with minimal disturbance to the neural networks there and deliver highly-controlled (spatially and temporally) charge waveforms to the tissue on a chronic basis. The probes consist of several thin-film conductors supported on a micromachined silicon substrate and insulated from it and from the surrounding electrolyte by silicon dioxide and silicon nitride dielectric films. The stimulating sites are activated iridium, defined photolithographically using a lift-off process. Passive probes having a variety of site sizes and shank configurations have been fabricated successfully and distributed to a number of research organizations nationally for evaluation in many different research preparations. For chronic use, the biggest problem associated with these passive probes concerns their leads, which must interface the probe to the outside world. Even using silicon-substrate ribbon cables, the number of allowable interconnects is necessarily limited, and yet a great many stimulating sites are ultimately desirable in order to achieve high spatial localization of the stimulus currents.

The integration of signal processing electronics on the rear of the probe substrate (creating an "active" probe) allows the use of serial digital input data which can be demultiplexed onto the probe to provide access to a large number of stimulating sites. Our goal in this area of the program has been to develop a family of 16-site active probes capable of chronic implantation in tissue. For such probes, the digital input data must be translated on the probe into per-channel current amplitudes which are then applied to the tissue through the sites. Such probes require five external leads, virtually independent of the number of sites used. As discussed in our previous reports, we have defined three probes which represent the first-generation of these active stimulating devices and have designated them as STIM-1, -1a, and -1b. All three probes provide 8-bit resolution in setting the per-channel current amplitudes over the biphasic range from $2\mu\text{A}$ to $\pm 254\mu\text{A}$; however, the probes differ markedly in the number of sites that can be active at any one time. STIM-1 offers the ability to utilize all 16 sites independently and in parallel, while -1a allows only two sites to be active at a time (bipolar operation), and -1b is a monopolar probe, allowing the user to guide an externally-provided current to the site selected by the digital address. The circuit complexity among these designs spans an order of magnitude in device count, ranging from a 400 transistors (STIM-1b) to over 7000 transistors (STIM-1). The high-end STIM-1 contains provisions for numerous safety checks and for features such as remote impedance testing in addition to its normal operating modes.

During the past quarter, research on this contract has focused on three areas. Two sets of new passive probes are currently in fabrication for both external and internal users, including a series of designs for penetration studies as described below. Efforts on the external instrumentation necessary to the testing of the probes is moving forward as well. In addition, the STIM-2 circuitry has been successfully operated with our external interface system, and a chip containing three versions of the STIM-2 probes has been designed. This chip contains reoptimized versions of STIM-1a and STIM-1b along with 8-shank and

16-shank versions of STIM-2. In addition, an 8-shank version of STIM-2 has been designed to allow a low probe implant profile to be retained above the cortex in chronic situations. The activities in these areas are described in the sections below.

2. Passive Stimulating Electrode Development

During the past quarter, two new mask sets of probes for both internal and external users were completed. These masks include both recording and stimulating designs, including probes for Huntington (Agnew), Rutgers (Buzsaki), and others. Also included are probes for the penetration studies described below. The probes embodied in these mask sets are now in process and are expected to be completed within the next three weeks. In addition, we have continued to fabricate probes from previous mask sets for our external users. Continuing intermittent adhesion problems are being experienced with the iridium metallization on our stimulating probes. These are sometimes so severe as to render a wafer useless, while at other times, even within the same run, the wafers appear free of the problem. It appears that the problem is localized between the iridium and the titanium undercoat and not between the titanium and the polysilicon interconnect since the poly is not attacked by the EDP silicon etchant used for final wafer dissolution. It is not clear how much of the problem is due to exceptionally high stress in the iridium and how much is due to relatively poor adhesion to the titanium, but these parameters are both being investigated. In addition, we have arranged to supply wafers to EIC Laboratories so that some sites can be inlayed with their iridium for comparison and so that they can characterize their iridium electrochemically on our polysilicon layers. These iridium problems have been in evidence for over two years in various degrees of severity, and we hope to discover the cause and correct it in the near future. We are also exploring the possibility of obtaining a sputtering system that can be dedicated to iridium deposition and to probe fabrication, eliminating any possibility of cross-contamination from other users.

2.1 Penetration Studies

As discussed in previous quarterly reports, a series of probes has been designed to study the insertion forces, long term probe-tissue coupling, and tissue damage associated with penetration through the pia arachnoid and dura mater in guinea pigs, rats and perhaps primates. These probes will be used to determine the optimal probe shank geometry which allows for ease of penetration with minimal cortical surface dimpling, minimal tissue damage and reaction along the insertion track, and maximal tissue-electrode coupling.

The six-layer mask set, PNTPROBES, for these probes was made in such a way as to allow fabrication of several different probe tip shapes by changing the fabrication steps slightly (see Table 1). The shallow boron masks are exactly the same except for their shapes at the tips of the probes (see Fig. 1, which also shows the layout configuration of the four point probe). Due to lateral diffusion during the deep boron diffusion, the dielectric mask keeps the shallow boron diffusion and final dielectric cut within the outline of the deep boron diffusion as layed out on some probes. Thus, it is the larger, more round shape of the deep boron diffusion profile that defines the probe tip. In contrast, the shallow boron mask on other tips allows the shallow boron diffusion and the final dielectric cuts to overlap the deep boron diffusion thus defining a much sharper tip profile as discussed in the previous quarterly report. Another option is to continue the final reactive ion etch (RIE) of the field dielectrics down through the boron diffusion of the probe tip to create a *quasi-chiseled* tip.

Step	Normal Process	Blunt Tip	Sharp Tip
1	Deep Boron	Deep Boron	Deep Boron
2	Shallow Boron	Dielectric*	Shallow Boron*
3	Polysilicon	Polysilicon	Polysilicon
4	Gold Pads	Gold Pads	Gold Pads
5	Iridium Sites	Iridium Sites	Iridium Sites
6	Dielectric	Dielectric**	Shallow Boron**

* lithographic image reversal

** optional deep RIE etch for quasi-chiseled tips

Table 1. Mask step order to realize the different tip geometries.

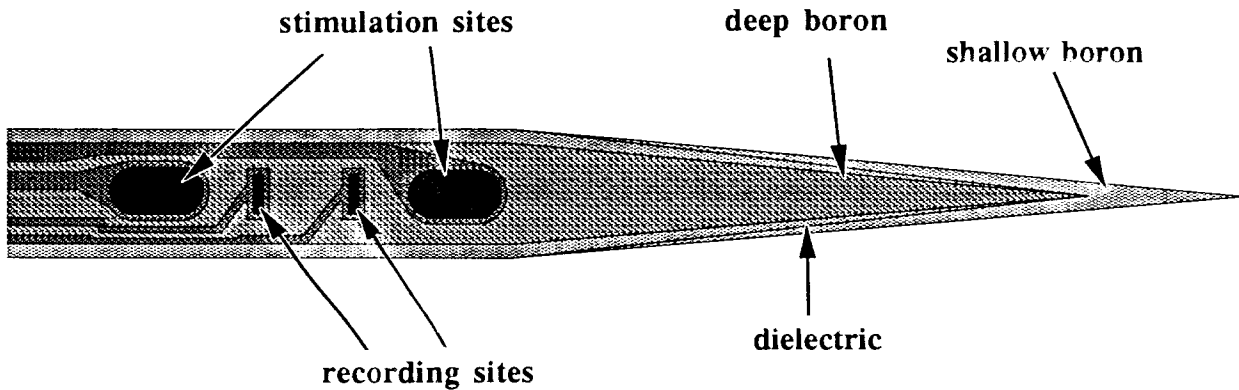


Fig. 1: The PSA1065 probe tip, demonstrating the masks for the two different tips and the the four point probe layout.

This masking pattern did require some deviation from a normal fabrication process in that it requires a lithographic image reversal for the dielectric/shallow boron masks at either the actual shallow boron diffusion or the final field dielectric cut. It was decided that the shallow boron diffusion lithographic step would be the image reversal step because it is a slightly more difficult to get good photoresist definition from image reversal and keeping in mind the option of creating quasi-chisel tips, the final field dielectric cut photoresist definition is more critical than the shallow boron diffusion.

The mask set included ten different probe designs. Table 2 lists the different probes and their important features and purpose. The overall probe shapes, shallow boron diffusion mask level, are shown in the layout of the mask die included in Fig. 2. The probe chronic_encapsul_1 will be used for the chronic recording vs. encapsulation evaluation by including four stimulation sites for the creation of artificial neural signals. This will be implanted in the inferior coliculus. The probe chronic_4_point will be implanted in the cortex to measure the tissue resistivity over time and thereby evaluate the expected initial fluid pooling around the probe shank and then the eventual reabsorption as the wound heals. An important feature of this probe is the 90° ribbon cable connection which gives the back area of the probe shank a very low profile. This has never been tried before and it is believed that the low profile and the ability for the ribbon cable to exit a distance from the probe will reduce the likelihood of the probe fusing to the cranium as the

wound heals. This allows the probe to *float* freely with the cortical surface as the brain pulsates reducing tissue reaction. The single shank probes with the varying widths and tip angles will be used to evaluate: penetration force (via their integrated polysilicon strain gauges), visual cortical surface dimpling, tissue damage, and recording ability, all versus tip shape or shank width. The three multi-shank probes each have three shanks with strain gauges (every second shank starting from the end), two shanks with two recording sites each (one outside shank and one interior shank), and five dummy shanks. These probes will be used to evaluate how shank separation and length tapering vary the penetration force, surface dimpling, and recording ability.

Fig. 2: Layout of the die for the PNTPROBES mask set, shallow boron mask level.

Table 2: List of probes and their descriptions.

in a guinea pig with some existing probes, coating them with the various stains and then evaluating the ease of finding the tracks. This knowledge will provide the basis for acute evaluation of the tissue damage caused by the various probe tip geometries.

This past quarter we have also begun to prepare the data acquisition system. LabView, a software development system produced by National Instruments, was purchased and installed on a Macintosh II and is being used to create the programs which will measure the strain gauge resistance and calculate the associated strain and longitudinal force in the probe shank, simultaneously perform frame-by-frame video capture of the tissue dimpling and penetration via a microscope with a video camera attached, and record the position of the probe from the microdrive. This keeps all of the different measurements time synchronized. LabView will also be used to produce the currents for the stimulation sites and record the voltage drop on the tissue resistivity tests. A constant current source/recording amplifier circuit was built to produce the actual driving currents from the computer D/A outputs and amplify the recorded voltage for the A/D inputs. Additionally, a software package called Video VI, produced by GTFS Inc., and an LG3 video digitizer card from Scion Corporation were purchased and installed on the Mac II. Video VI is a set of software tools, virtual instruments (VI's), specifically designed to support LabView in video capture from the LG3 video digitizer card, and in video display and analysis.

The PNTPROBES are currently being fabricated and will be completed during the coming quarter. The ongoing development of the data acquisition system and software is a top priority in this coming quarter as it will probably be the slowest part of the remaining experimental preparations.

2.2 External Interface Development

The past quarter has also been spent developing a system that will be used to run experiments during the fall and winter. These experiments will investigate how design parameters (e.g., stimulation site size) impact the stimulation capability of thin-film electrodes. The studies will be run on guinea pigs chronically implanted with passive stimulating electrodes. This report discusses the electrode implant, the components of the stimulation system, and one of the experiments that is currently being run.

The experiments we are presently performing use the three-shank, six-site, 1000 μm^2 per site probes described in previous quarterly reports (Fig. 3).

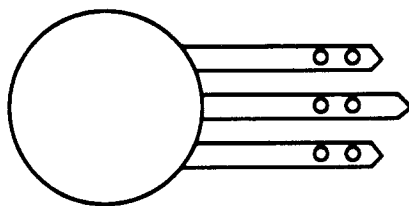


Fig. 3: Six site probe used for studies of the effect of site size on neural activation.

This electrode is implanted in the cochlear nucleus (CN) of the guinea pig. Two methods are used to record evoked response (ER) at later auditory pathways. One involves recording cortical auditory activity via two head screws. This response is used as a general assessment of the integrity of the implant. The second calls for implanting a wire recording

electrode in the brachium of the inferior colliculus (IC). We expect the IC implant to yield more quantitative results.

The system platform is a 486PC running the data acquisition program LabVIEW (National Instruments). LabVIEW is a graphical programming tool that allows the user to create algorithms for automated waveform generation and data acquisition, processing, and display. For this experiment, LabVIEW is programmed to repeatedly present a stimulus for a set amount of time. The stimulus is generated as a voltage output waveform from National Instruments I/O cards in the PC. An external circuit converts the voltage to a proportional current, which is then fed into the implanted animal (see Fig. 4). The circuit electrically isolates the electrode from the computer to reduce noise and ground loops.

The program will also take two types of data: one data set is a record of potential necessary to pass a specified current across the electrode sites; the second record is of the evoked response (ER) at some point further along in the auditory pathway. The access voltage data will be used to compute the impedance of electrode-animal system. The ER data will determine the effectiveness of the stimulation over time. Data collection can be triggered manually or automatically. Once the animal is connected, the system can be set up to run the entire test without user interaction.

The system will also be used to test electrode impedance *in vitro*.. Using the same I/O boards and the same external circuitry (plus a resistor network between the probe and the electronics), impedances can be tested for activated and inactivated probes.

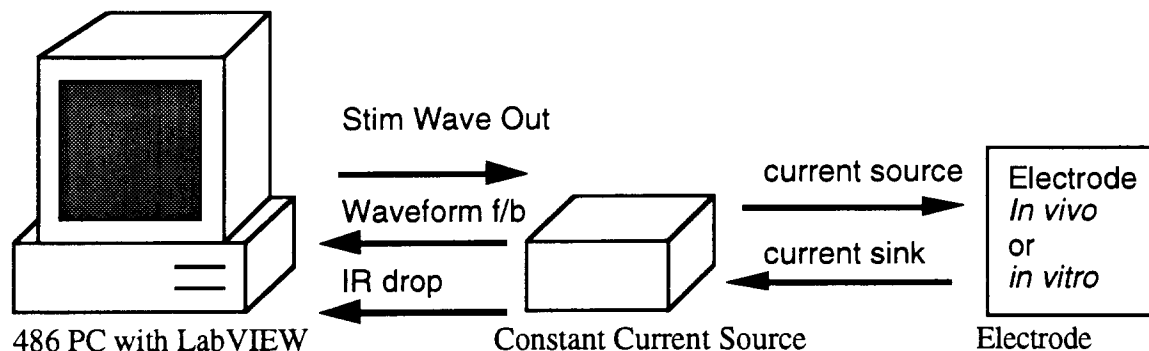


Fig. 4: Stimulation system

Stimulated neurons will express the protein CFos in abnormally high levels that remain elevated and even increase for a time after stimulation has ceased. An immunofluorescent label can then stain tissue samples and show which neurons were stimulated. CFos marking works at the cellular level, that is, only those cells that were stimulated will express CFos and hence will be stained. CFos tracing techniques are used in this experiment to provide some information about current flow between electrode sites in the cochlear nucleus and also to determine the level of response elicited in the inferior colliculus. Two types of stimulation will be performed and compared: between sites on the same shank (along shank) and between sites on different shanks (between shanks). It is hypothesized that, over time, there will be differences between the two directions of current flow due to the pattern of encapsulation.

The following guidelines are followed for the CFos experiment. The animal is implanted and electrode placement is verified by recording ER from head screws as mentioned above. Surgery is followed by a recovery period of 2-3 weeks. This time allows CFos levels, elevated by trauma from surgery, to return to nominal levels. To confirm this, several animals will be implanted but not stimulated. These will serve as controls. After the recovery period, electrode placement is again verified electrophysiologically. If the implant is intact, the animal is stimulated at a high level (150 μ A) for 90 minutes. CFos expression reaches its peak 2-4 hours after cessation of stimulation. Therefore, the animal is euthanized 2-4 hours after the stimulation ended. The animal is immediately perfused and the CN is sectioned. The sections are stained for CFos.

We are in the process of developing our experimental procedures for the CFos experiment. We hope to complete this work in the fall and begin long term stimulation tests in the winter.

Also in the area of instrumentation, we have been working to convert our handling of all real-time interactive experiments to LabVIEW. Both Mac and PC workstations are being used as the platform, depending on the experiment. An outline of the LabView programs which are being developed is given below with the status of each. Most of these are working in another form but are being converted to LabVIEW.

<i>Program</i>	<i>Function</i>	<i>Status</i>
Response Map	Takes up to 8 channels of auditory data and builds a rate vs. frequency and intensity plot for each channel	90% complete
Averaging	Simultaneously outputs a stimulus and collects data (1 ch.) for as many presentations as desired and averages the completely collected data and stores it in a file	complete
8 CH. collect	This program collects 8 channels of raw wave forms and stores it in a file, it also outputs any stimulus you want	80%
PSTH	Plot a histogram of the collected data depending on the trigger level chosen or depending on the clustering algorithm	Just getting started
Video capture	Collects video samples with other discrete-time samples such as deflection and force.	Just getting started
Impedance:	Tests all the sites of a probe for impedance with phase	80%

Table 3: Progress in converting real-time interactive experiments to LabVIEW.

3. Development of Active Stimulating Probes (STIM-2)

During the past quarter, we have designed and fabricated STIM-2 circuits through the chip-foundry, MOSIS. Most of the circuitry worked well as designed. Some weakpoints and layout errors in original design have been identified through thorough testing and corrected for the final versions (8-shank and 16-shank) of these stimulating probes. For reliable usage of such probes, some special issues (sharp probe tip, rounded probe edge, and flexible bending bridges between shanks and a probe body) have been

considered and implemented. In addition, the sequence of data designation reported before has been changed and will be briefly described in the following section.

In order to explore the development of these active probes, a probe mask set containing a wide variety of elements has been designed. The mask set (12-level masks) is designed for use with a $3\mu\text{m}$ p-well n-epitaxial ($16\mu\text{m}$ thick) single-poly double-metal two-step micromachined CMOS process with a die area of 155mm^2 as shown in Fig. 5. This chip consists of four modules. One of them is a test module designed for the characterization of individual circuit blocks and for the evaluation of the CMOS transistors and process parameters such as contact resistance, capacitance, and the sheet resistance of each layer, even after EDP etch. The rest are active probes, including modified STIM-1 versions (STIM-1A (bipolar) and STIM-1B (monopolar)) and STIM-2 (8-shank and 16-shank versions for fully-parallel operation). The chip is now being processed in our laboratory and will be finished in a few weeks. Its test results will be discussed in the next quarterly report.

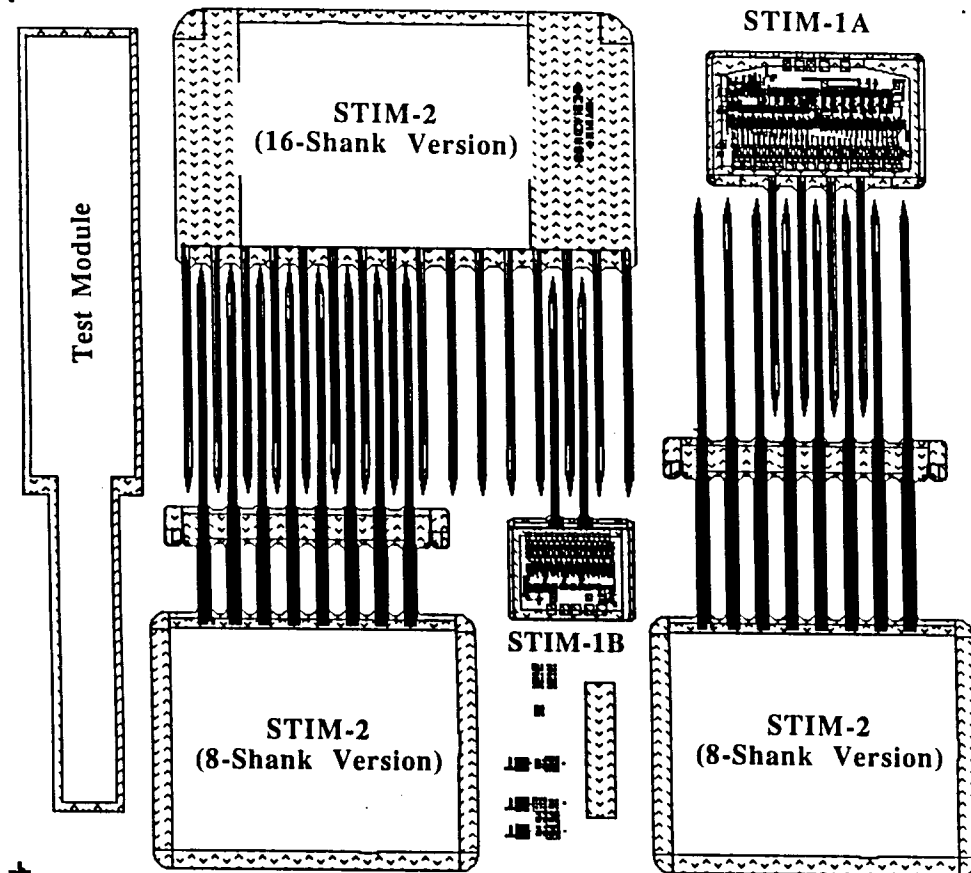


Fig. 5: Final layout for STIM-2. It contains a test module along with active probes STIM-1A, STIM-1B, and STIM-2 (8-shank and 16-shank versions) .

3.1 Second-Generation Active Stimulating Probe Designs

The ultimate goal of this research is to develop a second-generation active multishank (8 and 16) multisite (64 sites) neural microprobe for use in the central nervous system with the extendibility to three-dimensional assembly and with low-power on-chip circuitry. The electronic system designed for this probe will support 64 stimulating sites, simultaneously selecting any one of the 64 sites in both normal and special modes for either stimulation or recording. This selection scheme is globally multipolar since the time delay of 4 μ sec to select the next site is negligible at the clock frequency of 4.5MHz, appearing effectively simultaneous to the tissue. The probe allows stimulation through eight sites simultaneously, and any one of these sites can be monitored (recorded from) at any time. Table 4 shows a brief summary of the specifications and special features for the second-generation stimulating probe.

The system is configured as follows. Each group of eight electrodes, placed on a micromachined silicon probe shank, is connected to a front-end electrode selector (an 8-to-1 multiplexing array) and is controlled by a DAC. Up to one site from each group can be selected for monopolar current stimulation (globally, multipolar stimulation). For special options, several convenient modes are implemented, such as the site-activation mode, the site-impedance test mode, the neural recording mode, the low-impedance shunt mode for unactivated sites, the trouble flag mode, the current calibration mode, the anodic bias mode for high current delivery, and the platform address mode for three-dimensional arrays.

Table 4: Specifications of STIM-2

Process technology	3 μ m, p-substrate, n-epi, p-well single poly, double metal two-step diffusion micromachined CMOS technology
Supply voltage	V _{cc} = 5.0V, V _{ss} = -5.0V, GND = 0V
Control signals	DATA and CLOCK
Current range	-127 to +127 μ A
Current resolution	1 μ A
Power dissipation	Standby \leq 50 μ W, Operating \leq 10mW
Clock frequency	4.5 MHz (~222 nsec)
Time delay to select any site	4 μ sec
Total external pads	5 pads (3 powers, DATA, and CLOCK)
Electrode site size	1000 μ m ² (optional for 400 μ m ²)
Probe shanks	8 and 16
Total stimulating sites	64
Chip area with boundary	11.3 mm ²
Circuit features	<ul style="list-style-type: none"> • low-impedance shunt mode for idling sites • anodic-bias mode for high current delivery • electrode-impedance monitoring mode • electrode recording mode • self-test and trouble flag mode • electrode-activation mode • simple level-shifter with no static power • clock-controlled address decoder • low power current source (DAC)

Data Designations

A new detailed view of the timing and bit designations in STIM-2 is given in Fig. 6. The upper diagram illustrates the situation when normal data are transmitted as a 16-bit word instruction. A 16-bit word is serially clocked into the 8-bit serial shift register from the data line. The first 2 bits represent mode, followed by the six address bits. The first three of the address bits are decoded to select one of the eight DACs, and the second three bits are decoded to select one of eight sites associated with that DAC for simulation. During half of the ninth time slot, the data line sinks low to negative voltage signaling the mode and address latches to latch those bits. Eight bits of current data are then clocked in. These eight bits, representing the amplitude and sign of the sinking or sourcing currents, are directed into the level shifters. A strobe then occurs on the clock line, latching in these data, followed by the high impedance state that occurs during the last bit time, allowing the probe to transmit the "I'm OK" signal back to the external electronics. The remaining three possible combinations of modes are for recording (M01), low impedance shunt (M10), and extended data word (special mode) flag (M11). The lower portion of Fig. 6 illustrate the operation of a 32-bit instruction for cases which do not require high speed operation. Once again, the first and second parts of the address and the mode bits are clocked in and latched on the data strobe. At this time the mode bits are "11", indicating an extended instruction for special modes. In this case, the first three address bits in this first word are interpreted as special mode information and are latched to allow up to eight special modes. For example, at present the first four special modes are designated for anodic bias, impedance test, current calibration, and platform address as noted in Fig. 6. These could be used to address as many as 256 ($=2^8$) different probes in a distributed system, each probe having 64 sites. One special mode could be defined to allow a third data word as well, allowing the address space to be expanded further. The second 16-bit data frame is a standard probe command as used in a single instruction.

3.2 Special Considerations

For improved functionality and low power consumption, the second-generation active stimulating probe has been designed carefully and efficiently. The new probe contains a number of newly designed circuits and other features, including a negative pulse detector, a clock-controlled decoder with fewer transistors, a simple level shifter having no static power dissipation, wider lateral clearances around the p-wells to ensure freedom from lateral punchthrough and latch-up problems, and the use of wider metal for power buses. The next sections describe the important considerations for designing the second-generation probe. Using these considerations, high-performance active stimulating probes should be achieved.

Prevention of parasitic npn-BJT operation

We corrected a possible parasitic BJT operation which might occur in STIM-1 during the anodic-bias mode, in which the sites are biased one diode-drop above ground in order to achieve high charge delivery capability. Figure 7 shows a schematic diagram for parasitic npn-BJT operation that might occur during that mode, causing other parasitic BJT operations to be triggered as well.

Another method by which to achieve a diode-drop reference voltage for the anodic bias mode is to use a CMOS transistor in its saturation region so that such parasitic

operation can be eliminated completely. In the STIM-2 design, the latter method was implemented in order to ensure reliable circuit operation without parasitics.

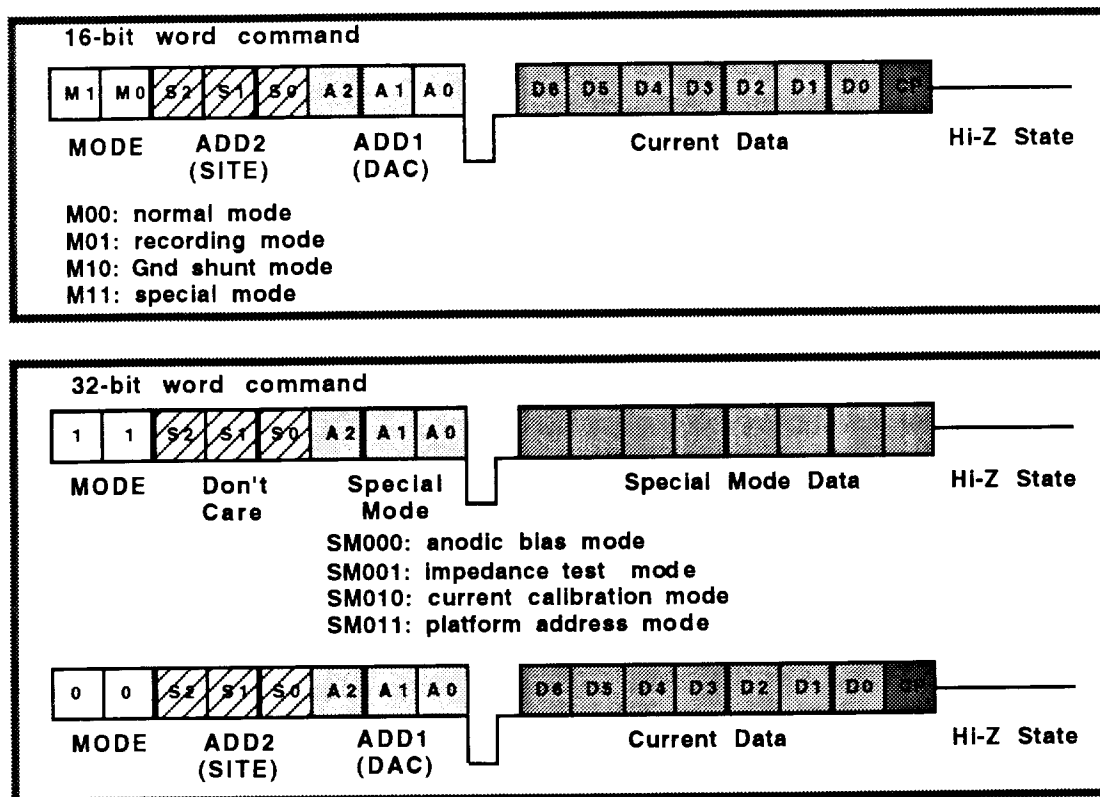


Fig. 6: Data designations for the second-generation stimulating probe.

Channel Selection and Stimulation Patterns

There are many useful combinations of stimulation patterns that could be used with sixty four sites. In order to allow a wide selection of these and yet maintain a reasonable level of complexity in the selection circuitry, a simple two-shank combination scheme has been chosen for STIM-2. Figure 8 shows a few of the possible stimulation patterns that can be implemented using this simple two-shank combination option. Each DAC can be switched to any one of eight sites that are distributed over two adjacent shanks. In this example, DAC1 controls sites 1-8, while DAC2 controls sites 9-16. This allows any two adjacent sites to be selected, for example, either laterally or in depth. A wide variety of patterns are possible, some of which are indicated in black in the probe silhouettes of Fig. 8. Figure 9 shows the physical probe shapes and site address maps for the 8-shank and 16-shank versions of STIM-2, respectively. Using this scheme, any two adjacent sites can be activated and used for bipolar stimulation.

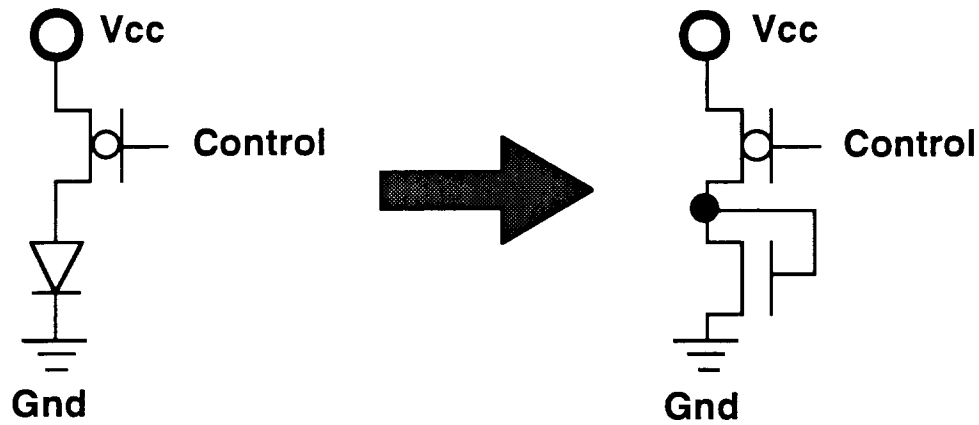
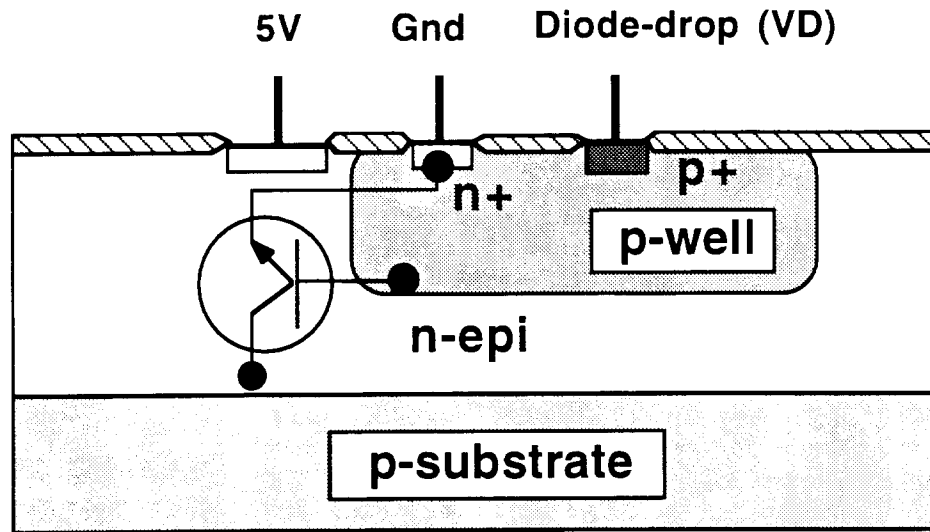


Fig. 7: Schematic diagram of parasitic npn-BJT operation during the anodic bias mode.

Probe Height Optimization

For the actual in-vivo application of these stimulating probes, their height above the cortex, which is determined by the circuit dimensions implemented in the probe, must be low enough to allow the dura to be folded back over the implant so that tissue overgrowth does not anchor the implant area to the skull. While the maximum allowable probe profile above cortex is not known at this time, it is assumed that this rise should be less than 1mm. However, as additional useful features are implemented on the probes, the chip size naturally increases, making a low profile increasingly difficult. While it is difficult to change the layout of the circuitry in order to physically reduce the overall chip height, it is possible to bend the probe so that the bulk of the circuitry lies flat against the cortex. The idea is that flexible bending bridges (implemented with the shallow boron diffusion used for the probe tips and cables) can be inserted between probe shanks and circuitry so that the circuit areas can be bent over against the circuitry. One of the versions of STIM-2 has been designed with this approach implemented as shown in the upper part of Fig. 9.

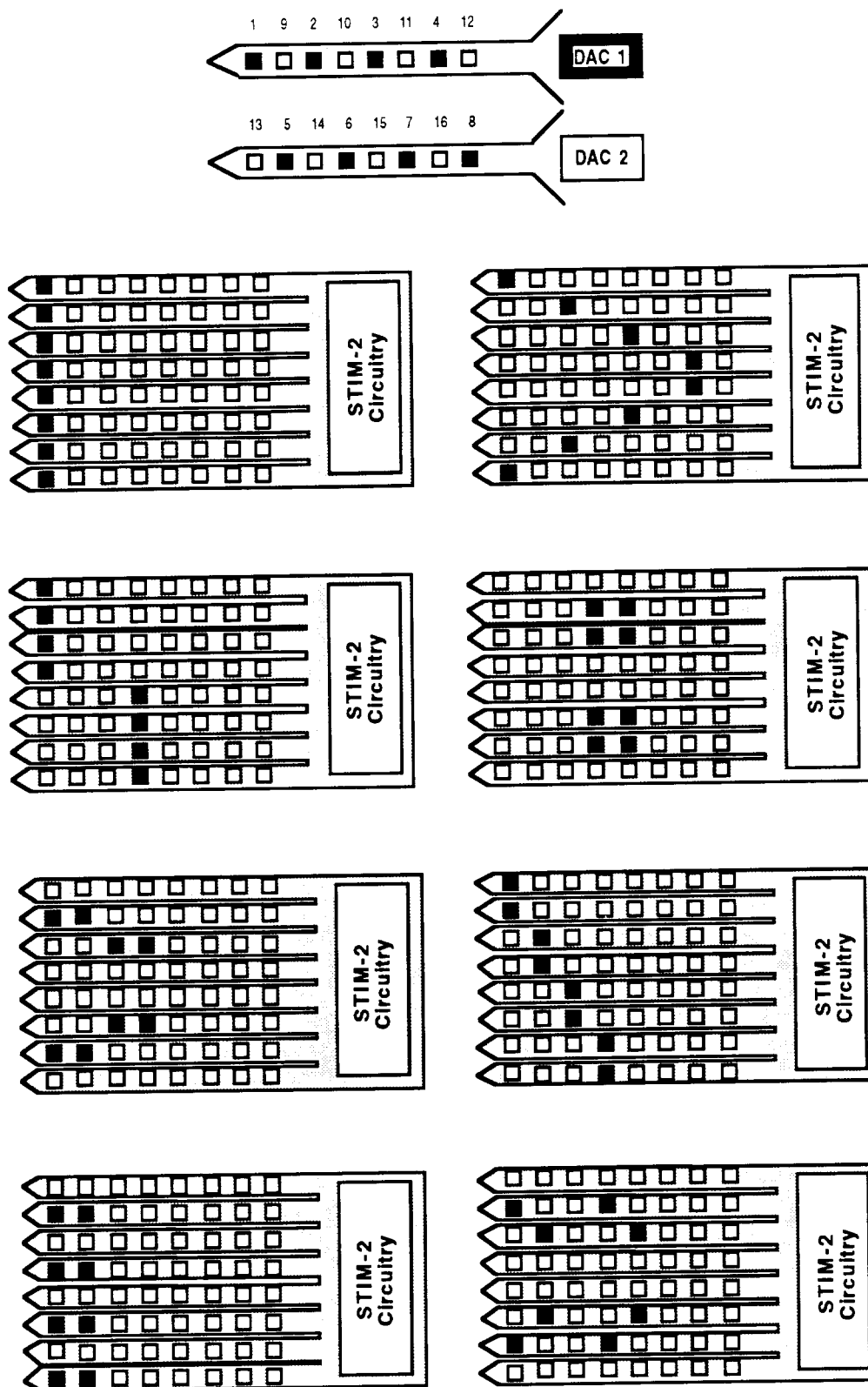


Fig. 8: Examples of possible stimulation patterns using a simple two-shank combination option for the organization of the DACs and the site selection matrix.

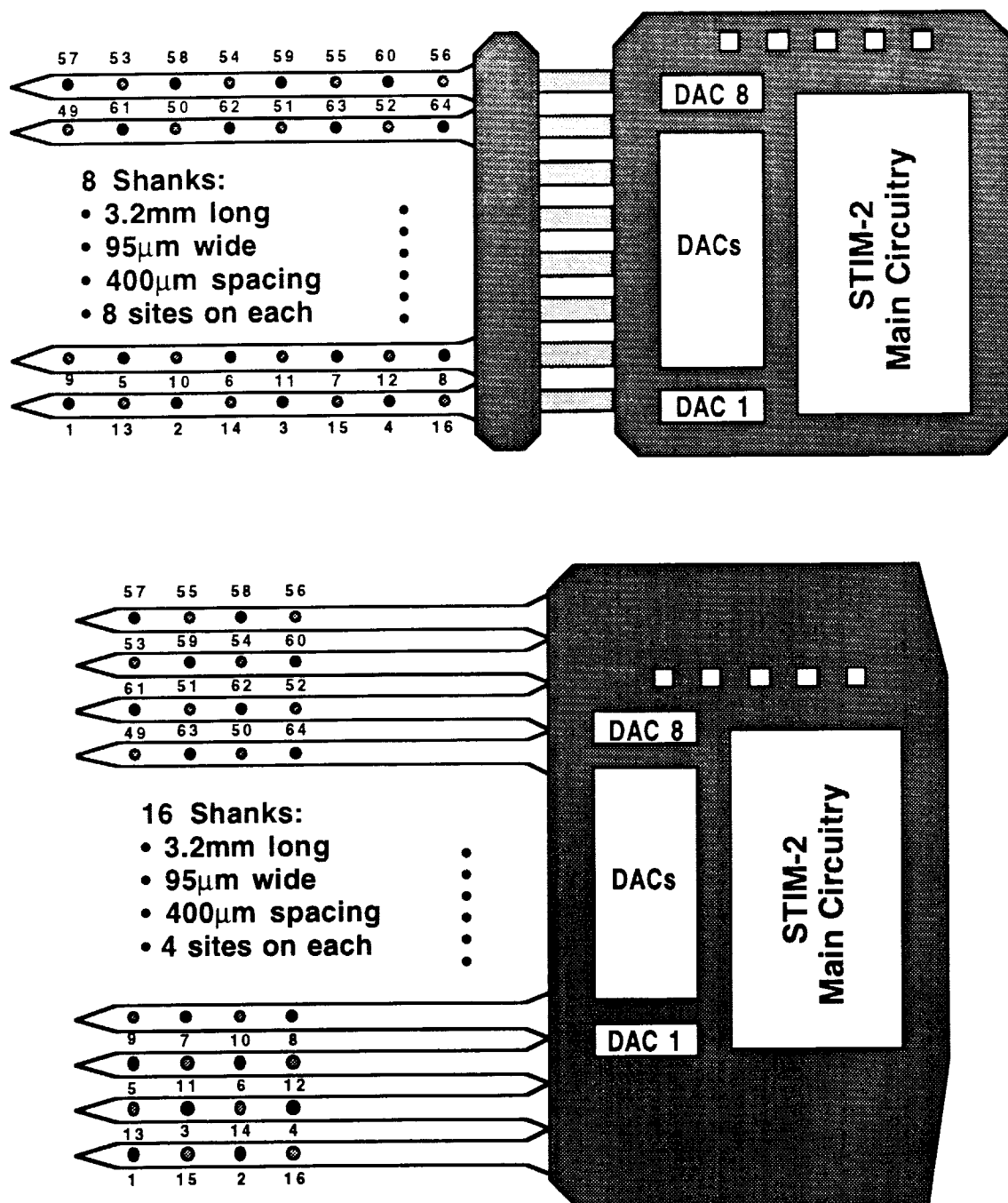


Fig. 9: Physical shapes and site maps of STIM-2. (a) 8-shank version (above) and (b) 16-shank version (below).

Experiments have been performed that show that slotted ribbon cables can be bent through arcs of 90° in radii of $<500\mu\text{m}$ quite reliably and with minimum tethering. In the layout of the bendable version of STIM-2, a first rear solid area has been left for handling that is about $350\mu\text{m}$ high. This portion of the device is slotted to make the structure compatible with use in a 3D array. The rear portion, containing all of the circuitry, is connected to this front-end over slotted cables 1mm long. The arrays can be prebent and held in position with a drop of polymer or can be placed and then stabilized with a suitable material on the cortical surface. In any case, this structure will be used for experiments involving chronic cortical placement of the arrays.

Prior to having the masks made for STIM-2, we operated the STIM-2 MOSIS circuit chips with our external computer-controlled interface for these devices. Fig. 10 shows the clock, data in, and output current from a representative site as the site current is stepped through its full-scale range from 0 to $+127\mu\text{A}$. The circuitry works satisfactorily with the interface. We expect to have the first samples of STIM-2 probes available by early fall.

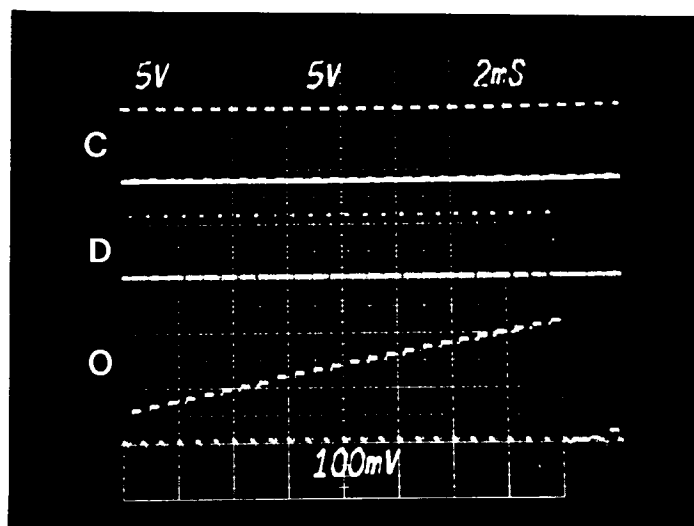


Fig. 10: Operation of STIM-2 circuitry with the external drive system developed for it. Top trace: input clock; middle trace: Data input: Lower trace: output current from a selected site.

4. Conclusions

During the past quarter, research under this program has gone forward in a number of areas. Passive probe fabrication has continued with new mask sets and probes for both external and internal users. Continuing problems with iridium stress and adhesion are being encountered on an intermittent but significant basis and are being investigated with the hope of understanding and eliminating them once and for all. The design of a mask set for probes aimed at optimizing tip shape for ease of insertion and for minimum tissue damage along the tracks has been completed, and the probes are now in fabrication. This set includes 10 different designs featuring a variety of tip angles and processes. Single probes, three-shank probes, and ten-shank probes are included along with strain gauges

mounted on some shanks for a direct measurement of entry forces. In parallel with these activities, work has gone forward to improve our external instrumentation for use with the probes. A visualization system has been implemented to enable cortical depression to be recorded, and all of the associated instrumentation for real-time interactive experiments in recording, stimulation, and strain-gauge monitoring has been converted to a LabView-based system. Penetration studies are expected to start in early October.

Using test results from STIM-1 and from STIM-2 circuit chips fabricated at the MOSIS foundry, we have corrected the process/design problems associated with STIM-1 and several minor design problems associated with the STIM-2 circuitry. During the past term, a chip containing the STIM-2 probes was designed, and the masks were fabricated. This chip contains modified layouts of STIM-1a (four-shank, 16-channel bipolar) and STIM-1b (two-shank 16-channel monopolar) as well as three versions of STIM-2: an eight-shank version, an eight-shank folding version, and a 16-shank version. All of the STIM-2 probes use the same circuitry, which implements 8 channels and a 64:8 front-end selector that allows those channels to be coupled to 64 iridium sites. The folding version uses slotted ribbon cables between the probe shanks and the circuitry to maintain a low profile above the cortex for chronic studies. All probes are designed for use with side-mounted ribbon cables. The masks for these devices have been received, and the STIM-2 probe wafers are currently in fabrication. The first prototypes are expected in October. In parallel with these activities, the circuitry for STIM-2 has been successfully operated with our external interface system, confirming the correct implementation of the interface protocols and other logic.